

Selected Papers from the 3rd Radiocarbon in the Environment Conference, Gliwice, Poland, 5–9 July 2021
© The Author(s), 2022. Published by Cambridge University Press for the Arizona Board of Regents on behalf of the University of Arizona. This is an Open Access article, distributed under the terms of the Creative Commons Attribution licence (<https://creativecommons.org/licenses/by/4.0/>), which permits unrestricted re-use, distribution, and reproduction in any medium, provided the original work is properly cited.

THE VERSATILE USES OF THE ^{14}C BOMB PEAK

Walter Kutschera* 

University of Vienna, Faculty of Physics – Isotope Physics, Waehringer Strasse 17, A-1090 Vienna, Austria

ABSTRACT. A concise review is presented of applying ^{14}C produced in the atmospheric nuclear weapons testing program (1950 to 1963), subsequently forming the so-called ^{14}C bomb peak. In order to convey the versatility of this unique isotope signal, selected applications from a variety of different fields are discussed touching on environmental, archaeological, biological, and forensic issues. A comprehensive list of references is supplied for in-depth studies of the respective fields.

KEYWORDS: biological and forensic applications, ^{14}C bomb peak dating, CO_2 cycle.

INTRODUCTION

It is well known that two anthropogenic contributions have influenced the natural $^{14}\text{CO}_2$ content in the atmosphere since the beginning of the 20th century. The emission of ^{14}C -free CO_2 from fossil fuel burning dilutes the ^{14}C content (Suess 1955), leading also to temporal variations of the interhemispheric ^{14}C offsets early in the 20th century (McCormac et al. 1998; Stuiver and Braziunas 1998). In contrast, atmospheric nuclear weapons testing after the second World War increased the ^{14}C content considerably (Figure 1).

In the late 1950s, a noticeable increase of ^{14}C was detected in the atmosphere and biosphere (Rafter and Ferguson 1957; De Vries 1958; Münnich and Vogel 1958; Broecker and Walton 1959; Broecker et al. 1959). Finally, the massive nuclear weapons testing in the early 1960s led to a sharp increase of ^{14}C , which peaked in 1963 (Nydal and Lövsøth 1965) when the limited Nuclear Test Ban Treaty ended this program. Since then, the anthropogenic excess of ^{14}C is gradually distributed from the atmosphere into the biosphere and hydrosphere. By now (2022) atmospheric $^{14}\text{CO}_2$ levels have reached almost pre-nuclear levels. This ^{14}C excess is called the “ ^{14}C bomb peak” and provides a distinct and rapidly changing ^{14}C signal for the past ~60 years (Levin and Hesshaimer 2000; Hua et al. 2013; Levin et al. 2022). Within this period ^{14}C “dating” with a time resolution of 1 to 2 years is possible. Since CO_2 emissions from fossil fuel burning will continue—albeit with hopefully decreasing intensity—a substantial depression below the natural level of the atmospheric $^{14}\text{CO}_2$ is predicted towards the end of the 21st century, shown in Figure 2 (Graven 2015).

The ^{14}C bomb peak was once colloquially called “The mushroom cloud’s silver lining” (Grimm 2008). This points out a positive side effect of the atmospheric nuclear weapons testing program. In essence, every carbon pool on Earth which was in exchange with atmospheric CO_2 since the late 1950s has been labeled by bomb ^{14}C (e.g., Bada et al. 1987). Combined with the extraordinary sensitivity of ^{14}C detection by AMS, allowing one to perform ^{14}C measurements in carbon samples down to the microgram range (Salehpour et al. 2015; Steier et al. 2017), has led to a large variety of applications. In the following, a limited number of representative examples will be discussed, demonstrating the versatile uses of the

*Corresponding author: Email: walter.kutschera@univie.ac.at

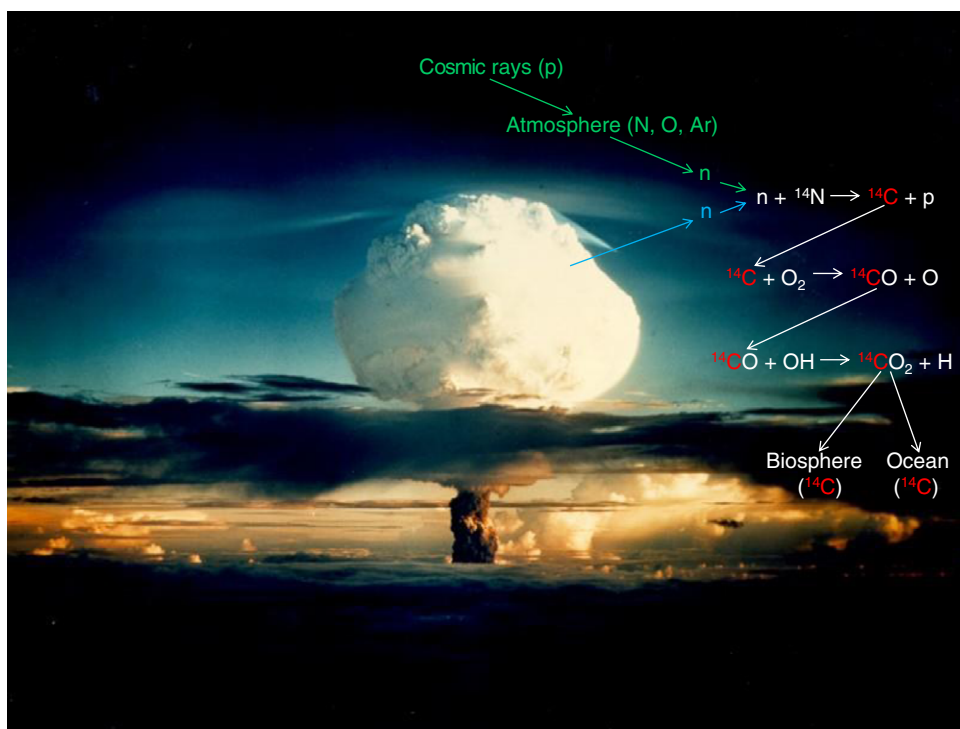


Figure 1 Schematic presentation of ^{14}C production from cosmic rays and nuclear explosions in the atmosphere and its pathway into terrestrial archives (Wild et al. 2019).

^{14}C bomb peak: (i) The uptake of anthropogenic atmospheric CO_2 into ocean and land. (ii) The age of groundwater systems. (iii) The study of annual tree ring growth in olive trees. (iv) The age of cells in the human body. (v) Other uses of the ^{14}C bomb peak in the biosphere. (vi) The evaluation of artwork with respect to its authenticity. (vii) The question of fraudulent whisky making. Although many uses of the ^{14}C bomb peak lead to a better understanding of basic processes in the environment at large (i–iv), it is also being used for forensic investigations elucidating the dark side of human beings (v–vii).

APPLICATIONS OF THE ^{14}C BOMB PEAK

The Uptake of Anthropogenic CO_2 into Ocean and Land

An important question for the development of the future climate on Earth is how much of the anthropogenic CO_2 released into the atmosphere can be taken up by oceans and land (plants and soil). We know that $\sim 45\%$ of it stays in the atmosphere, being monitored since more than 50 years at the Mauna Loa Observatory in Hawaii (Keeling 2008). The rest is taken up by the ocean ($\sim 25\%$) and land ($\sim 30\%$). However, to verify reported anthropogenic CO_2 emissions with independent Earth system observations, a better understanding of both contributions from natural variations in the CO_2 cycle and of the uptake processes is needed (Peters et al. 2017). These complex questions are being investigated from different angles for the oceans (Worden et al. 2015; Gruber et al. 2019), plants (Bastin et al. 2019; Slotta et al. 2021), and soil (Trumbore 2009; Shi et al. 2020). Here, the ^{14}C bomb peak provides a convenient tracer

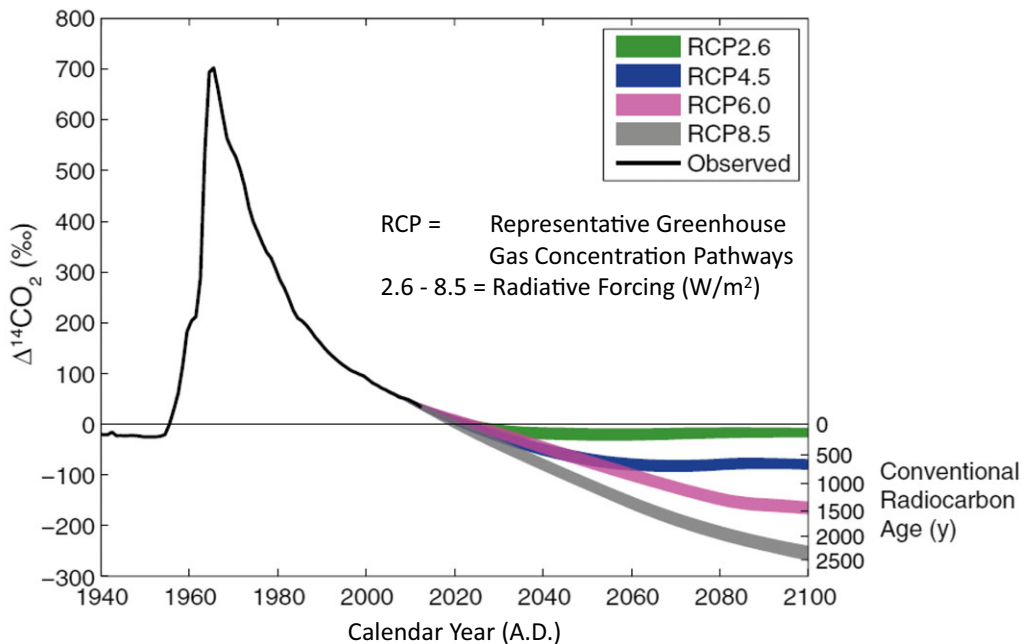


Figure 2 Modeling the impact of fossil fuel emissions in the 21st century on the anthropogenic “aging” of the atmosphere, depending on different scenarios of CO_2 reduction (Graven 2015). In the fifth assessment on climate change, the International Panel on Climate Change (IPCC 2013) used so-called Representative (greenhouse) Concentration Pathways (van Vuuren et al. 2011) to predict different radiative forcing values for 2100. Compared to an equilibrium between incoming radiation from space and outgoing radiation into space, positive radiation forcing values mean an increase of the temperature on Earth. A continuation of “business-as-usual” results in a radiative forcing of $8.5 \text{ W}/\text{m}^2$ in 2100 and the most negative $\Delta^{14}\text{CO}_2$ values (gray curve).

to study decadal dynamics of CO_2 , whereas cosmogenic ^{14}C is useful at the millennium time scale.

As an interesting example, we show the surprising penetration of bomb ^{14}C into the deepest regions of the oceans (Wang et al. 2019), depicted in Figure 3.

The Age of Groundwater Systems

Groundwater is the largest freshwater resource on earth. Since our life depends on the availability of freshwater, it is important to understand the residence time of a groundwater system (Seltzer et al. 2021), and how fast it is being recharged by precipitation. The age of groundwater systems can provide a first estimate of this information.

Very old groundwater system such as the Great Artesian Basin in Australia have ages around several hundred thousand years (Collon et al. 2000). They are being continuously depleted by human use, with expected very long recharging times.

Here we give an example of a likely short recharging time established by ^{14}C bomb peak dating of young speleothems in a groundwater system about 100 km from Sydney (Hodge et al. 2011).

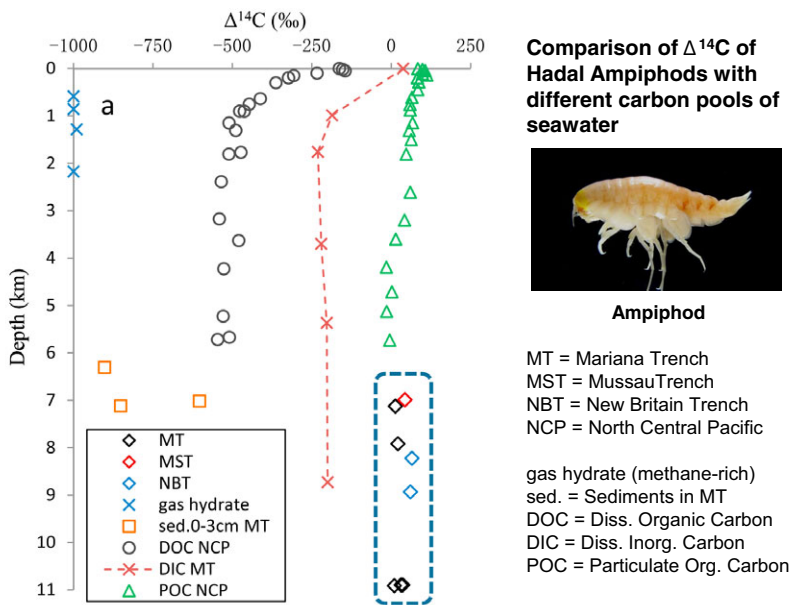


Figure 3 Penetration of ^{14}C bomb signal into the deepest trenches of the western Pacific Ocean (Wang et al. 2019), found by measuring $\Delta^{14}\text{C}$ in Hadal Ampiphods who live there (diamond symbols within the area encircled by the dashed line). This indicates a rapid exchange of particulate organic carbon (POC) with the deepest regions of the oceans. For comparison, $\Delta^{14}\text{C}$ measurements of organic and inorganic material in the oceans as a function of depth are also displayed (non-diamond symbols).

Only a 5-year shift occurs between the atmospheric ^{14}C bomb signal and the one recorded in a fast growing stalagmite (Figure 4). Thus, a short recharging time is likely to be expected.

In general, however, in a cave system there are different water pathways for different stalagmites, depending on their locations in the cave and the overlaying rocks and soil. It is therefore a complex undertaking to come up with good estimates of the groundwater recharging times for different cave system (Markowska et al. 2019).

The Study of Annual Tree Ring Growth in Olive Trees

An exact date of the Late Bronze Age eruption (~1600 BCE) on the Greek island of Santorini in the Aegean Sea is of great interest to archaeologists and historians studying the interaction of different civilizations in the Eastern Mediterranean during that time (Warren 2006; Kutschera 2020). Great efforts have been made to determine this date by ^{14}C dating. A key object was a branch of an olive tree supposedly buried alive in the tephra from the volcanic eruption (Friedrich et al. 2006). A detailed tree-ring study of a modern olive tree with the help of the ^{14}C bomb peak (Ehrlich et al. 2018, 2021) revealed a complex tree ring growth pattern, raising doubts on the reliability of using olive trees for ^{14}C dating (Figure 5). In addition, a new year-to-year ^{14}C calibration (Pearson et al. 2018) established a critical shift in the “plateau” region between 1600 and 1500 BCE, which does not allow one to obtain a precise date within this time range from ^{14}C measurements. It seems that other dating methods need to be used to determine an accurate date for this important time beacon (Kutschera 2020).

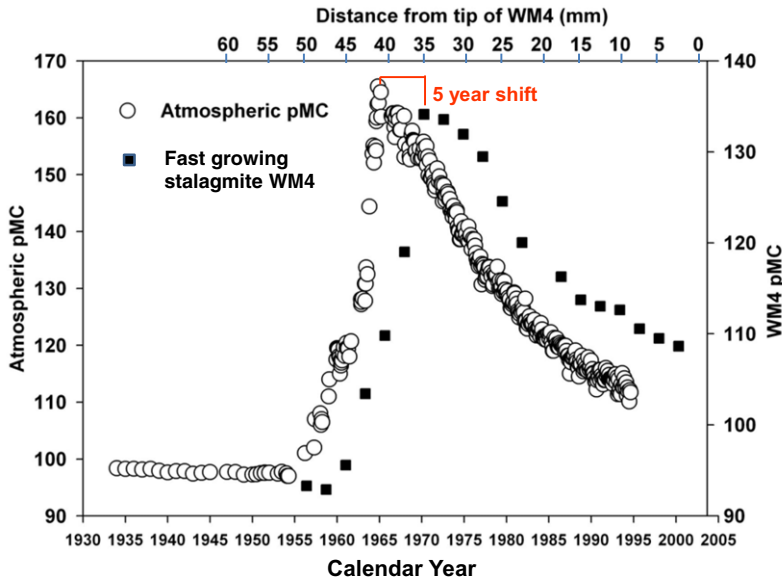


Figure 4 The figure shows a ~5-year shift between the atmospheric ^{14}C bomb peak and the same signal recorded in a fast-growing stalagmite (Hodge et al. 2011), indicating a short recharging time of this groundwater system.

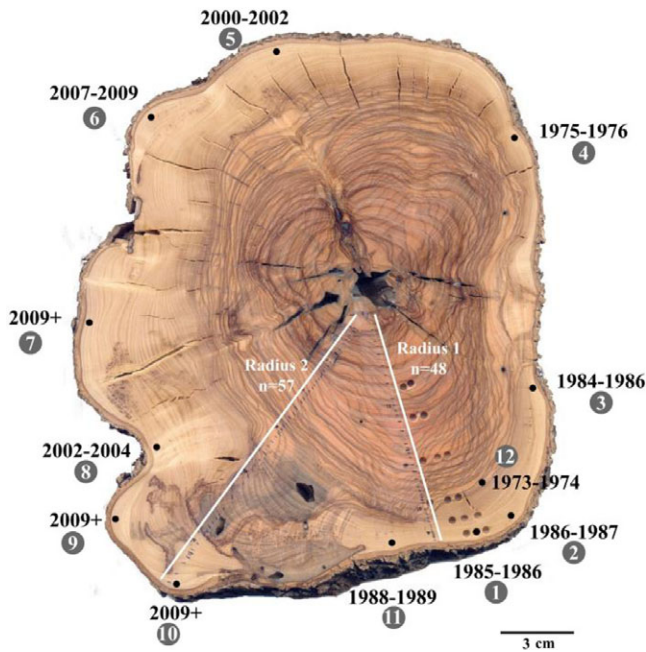


Figure 5 Cross section of a modern olive tree from northern Israel cut in 2013, where ^{14}C bomb peak measurements around the circumference revealed a considerable variation of ages (Ehrlich et al. 2018). Only those regions marked with 2009+ gave signals consistent with the year of the cutting. Up to 40-year older ages are observed (point 4).

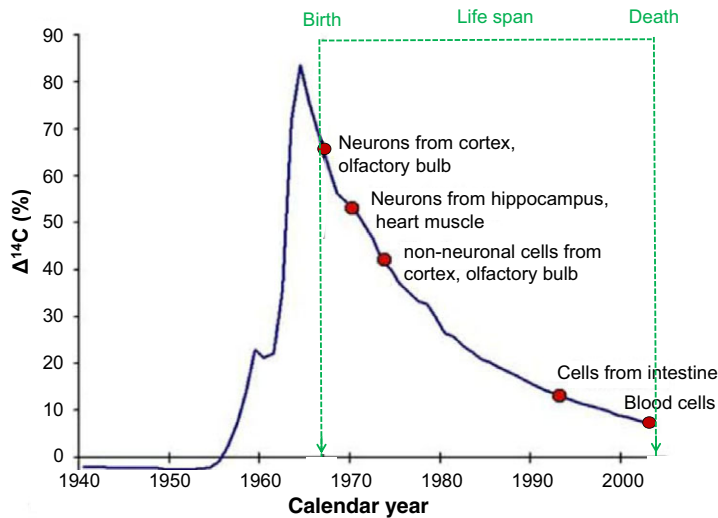


Figure 6 Visualization of how the birth date of different cells in an individual of a known life span can be determined retrospectively by comparing the measured ^{14}C signal from DNA extracts with the ^{14}C bomb peak calibration curve (Spalding et al. 2005).

The Age of Cells in the Human Body

One of the most fascinating applications of the ^{14}C bomb peak was developed by the Department of Cell and Molecular Biology of the Karolinska Institute in Stockholm, based on the following hypothesis, quoted from their seminal paper (Spalding et al. 2005): “Most molecules in a cell are in constant flux, with the unique exception of genomic DNA, which is not exchanged after a cell has gone through its last division. The level of ^{14}C integrated into genomic DNA should thus reflect the level in the atmosphere at any given point, and we hypothesized that determination of ^{14}C levels in genomic DNA could be used to retrospectively establish the birth date of cells in the human body.” All humans who lived during the time of the bomb peak are thus potential objects for these studies (Figure 6).

The formation of new neurons after birth is of particular interest for the human brain. Here we show one striking example. Evidence for the formation of new neurons after birth were found in the hippocampus, an important part of the human brain where memory forming, organizing, and storing takes place (Spalding et al. 2013). The result of this investigation is displayed in Figure 7. In contrast, essentially no renewal of neurons after birth was found in other sections of the human brain, the neocortex (Bhardwaj et al. 2006) and the olfactory bulb of the human brain (Bergmann et al. 2012). The age and genomic integrity of neurons after cortical strokes has also been investigated (Huttner et al. 2014). In general, the ability of the human brain to adapt to changing conditions (so-called “neuroplasticity”) is a field of intense studies (Yeung et al. 2014; Frisén 2016).

The method has also been extended to study cells in the human heart (Bergmann et al. 2009), delivering information about constancy and renewal rates of different cells, important to a

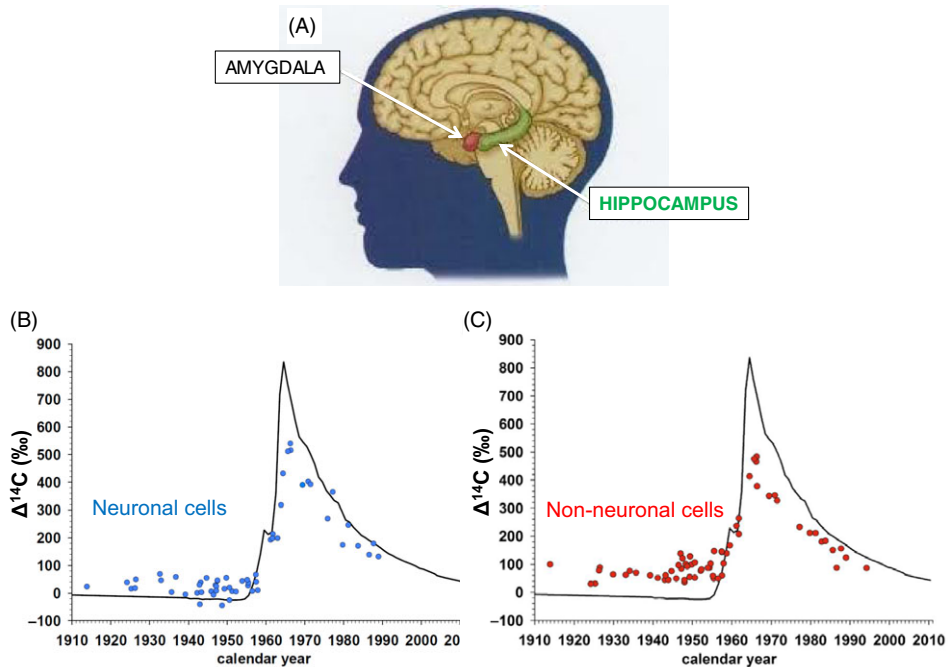


Figure 7 Evidence for neurogenesis in the human hippocampus (Spalding et al. 2013). $\Delta^{14}\text{C}$ values of neuronal and non-neuronal cells from the hippocampus (A) are plotted at the respective birth dates of 57 individuals (B and C). Deviations from the ^{14}C bomb curve indicate the formation of new cells after birth. The offset between the atmospheric bomb curve and DNA measurements is indicative of the magnitude of cell turnover. The smaller offset of neurons indicates their turnover is smaller than non-neurons.

reliable functioning of the heart (Bergmann et al. 2015). Another application of considerable health impact is the study of the turnover of fat cells (adipocytes) since obesity increases in many countries around the world (Spalding et al. 2008; Arner et al. 2011; Hyvönen and Spalding 2014; Arner et al. 2019).

Other Uses of the ^{14}C Bomb Peak in the Biosphere

Timing of Birth and Death

The time of birth of humans can be determined by measuring bomb ^{14}C in parts of the body where carbon is not exchanged after birth. Examples are the enamel of teeth (Spalding et al. 2005; Buchholz and Spalding 2010), and in the eye lens crystalline (Lynnerup et al. 2008; Kjeldsen et al. 2010). In a refined ^{14}C bomb-peak study, the separation of water-soluble and insoluble proteins of the human lens showed that the latter forming the crystalline core of the lens exhibited very low level of new carbon incorporation/exchange/turnover (Stewart et al. 2013). A particularly detailed study of the age distribution of tissue in the human eye was performed by the AMS group in Debrecen (Rinyu et al. 2020).

The time of death of a human can be of forensic interest. It can be determined from measuring ^{14}C in material that has been renewed as close to the death of the person as possible, i.e., lipid

fraction of bones, or hair (Wild et al. 1998). In a court case, where two old women were found dead in an apartment, a time difference of ~ 1 year for the time of death for the two individuals could be established (Wild et al. 1998).

Longevity of Sharks

Sharks are iconic species in the animal world of the oceans, and the age of some great white sharks (*Carcharodon carcharias*) has been determined with ^{14}C bomb peak dating of banded vertebrae to be as high as 70 years (Hamady et al. 2014). In a similar study of banded vertebrae in whale sharks (*Rhincodon typus*), the largest fish in the world, ages of up to 50 years were determined (Ong et al. 2020). An even greater age has been found for Greenland sharks (*Somniosus microcephalus*), with a maximum age of 400 years (Nielsen et al. 2016). The latter was established with the eye-lens dating method mentioned above.

African Elephants and Ivory Trade

A comprehensive description of the use of the ^{14}C bomb peak for the measurement of recent biological tissues and application to wildlife forensics can be found by Uno et al. (2013). In the land animal world, African elephants can also be considered iconic species. Their killing has been prohibited since 1989 by CITES (The Convention on International Trade in Endangered Species of Wild Fauna and Flora). However, since their tusks provide valuable ivory, they are still being hunted after the ban. In a big effort to uncover illegal trade of ivory, the ages of large ivory seizures were determined with ^{14}C bomb peak dating (Cerling et al. 2016). In the abstract they state: “Carbon-14 measurements on 231 elephant ivory specimens from 14 large ivory seizures (≥ 0.5 ton) made between 2002 and 2014 show that most ivory (ca. 90%) was derived from animals that had died less than 3 years before ivory was confiscated” (Figure 8). This is in clear violation of the CITES convention and revealed the relentless poaching of elephants in Africa (Wasser et al. 2015; Biggs et al. 2017).

Another study related to ivory and forensics was performed by the AMS group at the University of Salento, Italy, where also tusks from mammoths were investigated (Quarta et al. 2019). In a more positive application of the ^{14}C bomb peak, six privately owned tusks from African elephants, supposedly from before the ban from CITES, were clearly confirmed to belong to elephants hunted in the 1960s (Wild et al. 2019).

The Authenticity of Artwork

It is probably not an exaggeration to say that the preservation of cultural heritage is a key to understand the development of different cultures from the past to their present state, and that it may contribute to a more respectful interaction between cultures. Part of this includes artwork, and often they gain considerable value if an authenticity can be proven by scientific methods. The development of ^{14}C dating with AMS allows one to make such measurements on artwork with very small samples. However, great care needs to be taken to identify the origin of the object to be ^{14}C dated, because, unfortunately, looting and forging is not uncommon on the art market (Huysecom et al. 2017; Hajdas et al. 2019).

Here, we give an example where the authenticity of a painting by a French artist was checked by applying ^{14}C bomb peak dating (Caforio et al. 2014). It turned out that the painting, which supposedly was produced by the artist early in the 20th century, actually originated from a time period when the artist was already dead. This was proven by finding a ^{14}C signal in a small sample from the canvas of the painting, which clearly showed the ^{14}C excess from the ^{14}C

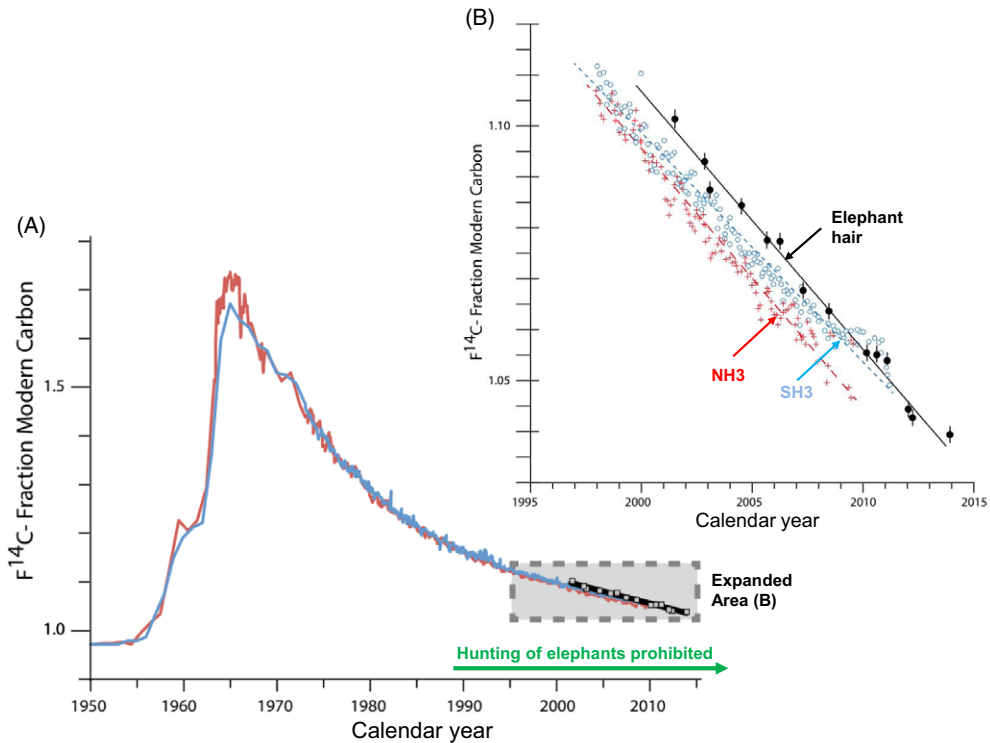


Figure 8 ^{14}C bomb peak calibrations from the investigation of illegal ivory trade (Cerling et al. 2016). NH3 (red color) and SH3 (blue color) are calibration curves for the Northern and Southern Hemispheres, respectively (Hua et al. 2013). To determine a correct age of the elephant tusks, a calibration curve was established for the time period 2001 to 2013 from ^{14}C measurements of elephant hair at known collection dates (B). The offset between the atmosphere and the elephant hair reflects the time lag of building up the keratin in hair from the foot stuff (plants, grass) consumed by the elephants. For calibration purposes, hair is assumed to be the best representative of the keratin in ivory (Cerling et al. 2016). (Please see electronic version for color figures.)

bomb peak (Figure 9). In this case, it was fairly easy to show that the painting must have been a fake.

The Question of Fraudulent Whisky-Making

Scotch whiskies are world-renowned products whose original year of production is of great importance for connoisseurs and collectors. In an elaborate effort at the SUERC AMS facility near Glasgow, the Northern Hemisphere ^{14}C bomb peak calibration curve NH1 (Hua et al. 2013) was verified closely by measuring ^{14}C in the ethanol component of 221 single malt whisky samples of known distillation year (Figure 10A). The observed ca. 1-year offset is consistent with the time between barley harvest and distillation (Cook et al. 2020). This “whisky” calibration curve from 1950 to 2015 was then used to examine a range of whiskies supposedly distilled over the last 150 years. Some were found to be genuine, but others were clearly identified to be fakes (Cook et al. 2020). For these conclusions it was also important to measure $\delta^{13}\text{C}$ values for the samples, since the slow

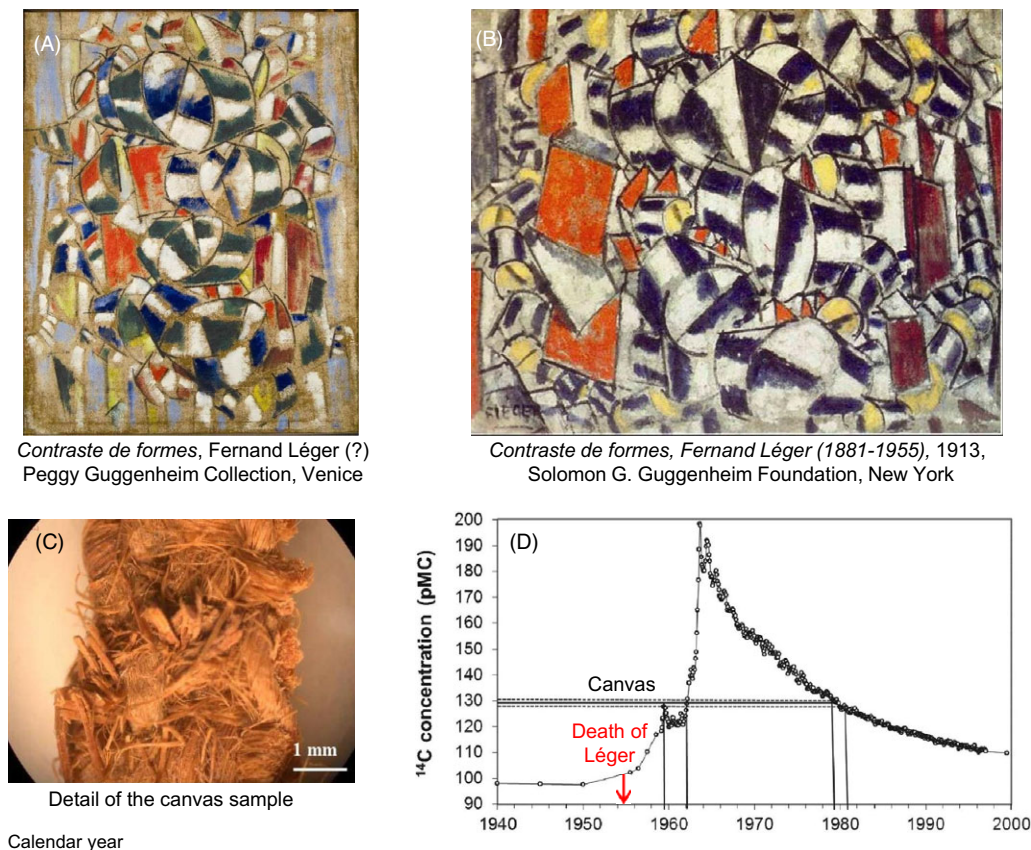


Figure 9 Measurement of ^{14}C from a small piece of canvas (C) from the back of a painting possibly made by Fernand Léger (A) and of similar appearance than the one definitely belonging to this artist (B). It revealed a date after the death of Léger (D), proving it to be a fake (Caforio et al. 2014).

decrease with time due to the atmospheric CO_2 contribution from fossil fuel burning provided an additional signature to fix the year of the distillation (Figure 10B).

CONCLUSION

The current review of the versatile uses of the ^{14}C bomb peak could only touch an a few specific examples. Nevertheless, it should have made it clear that ^{14}C from the atmospheric nuclear weapons testing program entered the entire world through the CO_2 cycle in the second half of the 20th century. In particular, the entire biosphere on Earth including humans, animals, and plants who lived through this time period is labeled with an excess of ^{14}C . This allows unique studies of dynamic processes on decadal time scales, including also the important question of how much of the anthropogenic CO_2 is taken up in various reservoirs on Earth. It is likely that many more studies will be conducted benefitting from the ^{14}C bomb signal which, however, will be “washed out” in the 21st century. There, the continued emission of “dead” CO_2 from fossil fuel burning will lead to a marked suppression of the ^{14}C signal below the natural level (Graven 2015).

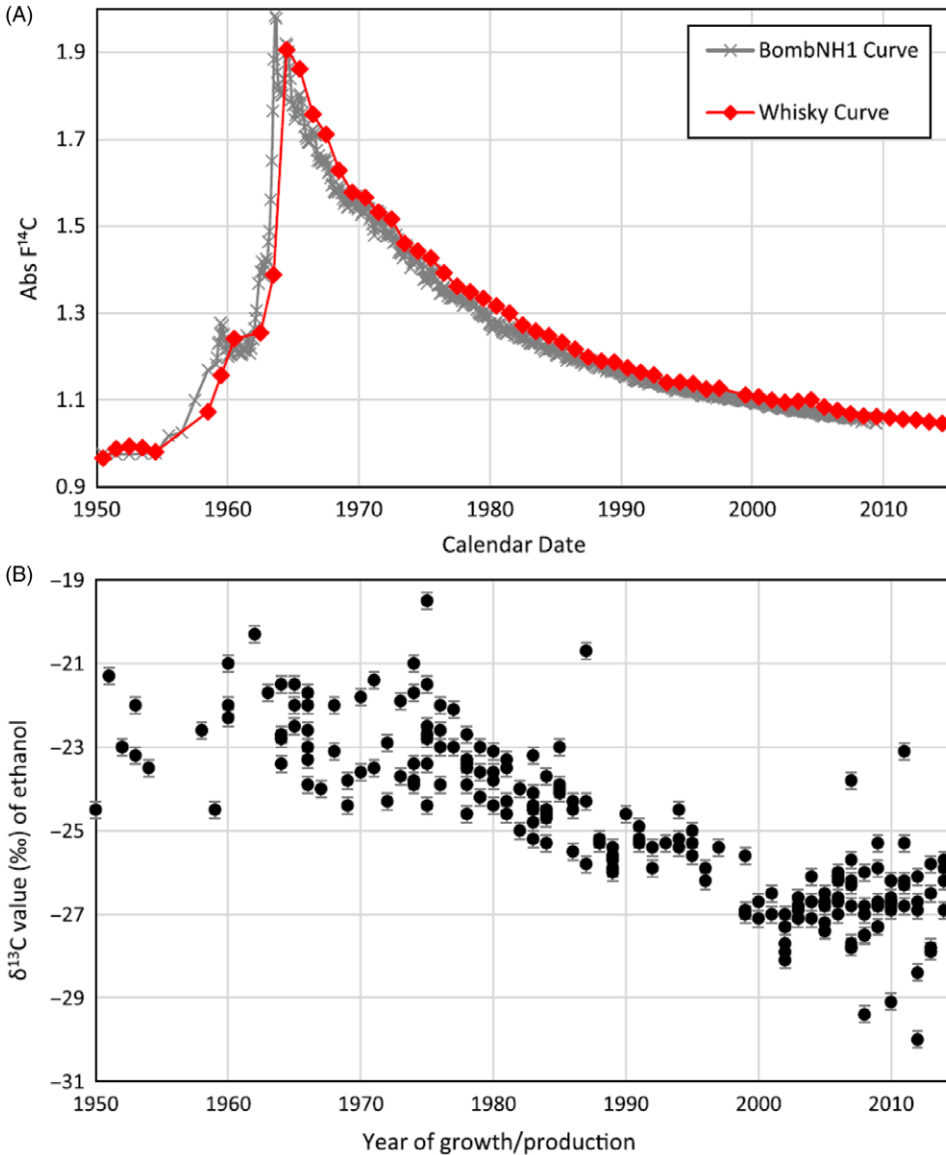


Figure 10 ^{14}C calibration curve from known-age whiskies closely resembles the atmospheric ^{14}C bomb curve (A). The lower part of the figure displays the $\delta^{13}\text{C}$ values of the ethanol from these whisky samples (B). Together, these two carbon isotope signatures allowed one to determine the true age of valuable whiskies, and to distinguish between genuine products and fakes (Cook et al. 2020).

ACKNOWLEDGMENT

The author acknowledges helpful discussions with colleagues around the world who had particular expertise in the respective fields described in this review. Detailed comments from two reviewers on the original manuscript are also gratefully acknowledged.

REFERENCES

- Arner P, Bernard S, Appelsved L, Fu K-Y, Anderson DP, Salehpour M, Thorell A, Rydén M, Spalding KL. 2019. Adipose lipid turnover and long-term changes in body weight. *Nature Medicine* 25(9): 1385–1389.
- Arner P, Bernard S, Salehpour M, Possnert G, Liebl J, Steier P, Buchholz BA, Eriksson M, Arner E, Hauner H, Skurk T, Rydén, Frayn KN, Spalding KL. 2011. Dynamics of human adipose lipid turnover in health and metabolic disease. *Nature* 478:110–113.
- Bada JL, Vrolijk CD, Brown S, Druffel ERM, Hedges REM. 1987. Bomb radiocarbon in metabolically inert tissues from terrestrial and marine mammals. *Geophysical Research Letters* 14(10):1065–1067.
- Bastin J-F, Finegold Y, Garcia C, Mollicone D, Rezende M, Routh D, Zohner CM, Crowther TW. 2019. The global tree restoration potential. *Science* 365:76–79.
- Bergmann O, Bhardwaj RD, Bernard S, Zdunek S, Barnabé-Heider F, Walsh S, Zupicich J, Alkass K, Buchholz BA, Druid H, Jovinge S, Frisén J. 2009. Evidence for cardiomyocyte renewal in humans. *Science* 324: 98–102.
- Bergmann O, Liebl J, Bernard S, Alkass K, Yeung MSY, Steier P, Kutschera W, Johnson L, Landén M, Druid H, Spalding KL, Frisén J. 2012. The Age of olfactory bulb neurons in humans. *Neuron* 74:634–639.
- Bergmann O, Zdunek S, Felker A, Salehpour M, Alkass K, Bernard S, Sjöstrom SL, Szewczykowska M, Jakowska T, dos Remedios C, Malm T, Andrä M, Jashari R, Nyengaard JR, Possnert G, Jovinge S, Druid H, Frisén J. 2015. Dynamics of cell generation and turnover in the human heart. *Cell* 161:1566–1675.
- Bhardwaj RD, Curtis MA, Spalding KL, Buchholz BA, Fink D, Björk-Eriksson T, Nordborg C, Gage FH, Druid H, Eriksson PS, Frisén J. 2006. Neocortical neurogenesis in humans is restricted to development. *Proceedings of the National Academy of Sciences USA* 103:12564–12568.
- Biggs D, Holden MH, Braczkowski A, Cook CN, Milner-Gulland EJ, Phelps J, Scholes RJ, Smith RJ, Underwood FM, Adams VM, Allan J, Brink H, Cooney R, Gao Y, Hutton J, Macdonald-Madden E, Maron M, Redford KH, Sutherland WJ, Possingham HP. 2017. Breaking the deadlock on ivory. *Science* 358:1378–1381.
- Broecker WS, Schulert A, Olson EA. 1959. Bomb carbon-14 in human beings. *Science* 130: 331–332.
- Broecker WS, Walton A. 1959. Radiocarbon from nuclear tests. *Science* 130:309–314.
- Buchholz BA, Spalding KL. 2010. Year of birth determination using radiocarbon dating of dental enamel. *Surface and Interface Analysis* 42:398–401.
- Caforio L, Fedi ME, Mandò PA, Minarelli F, Peccenini E, Pellicori V, Petrucci FC, Schwartzbaum P, Taccetti F. 2014. Discovering forgeries of modern art by the bomb peak. *European Physical Journal Plus* 196:6.
- Cerling TE, Barnette JE, Chesson LA, Douglas-Hamilton I, Gobush KS, Uno KT, Wasser SK, Xu X. 2016. Radiocarbon dating of seized ivory confirms rapid decline in African elephant populations and provides insight into illegal trade. *Proceedings of the National Academy of Sciences USA* 113(47):13330–13335.
- Collon P, Kutschera W, Loosli HH, Lehmann BE, Purtschert R, Love A, Sampson L, Anthony D, Cole D, Davids B, Morrissey DJ, Sherrill BM, Steiner M, Pardo RC, Paul M. 2000. ^{81}Kr in the Great Artesian Basin, Australia: a new method for dating very old groundwater. *Earth and Planetary Science Letters* 182:103–113.
- Cook GT, Dunbar E, Tripney BG, Fabel D. 2020. Using carbon isotopes to fight the rise in fraudulent whisky. *Radiocarbon* 62(1):51–62.
- De Vries H. 1958. Atomic bomb effect: variation of radiocarbon in plants, shells, and snails in the past 4 years. *Science* 128:250–251.
- Ehrlich Y, Regev L, Boaretto E. 2018. Radiocarbon analysis of modern wood raises doubts concerning a crucial piece of evidence in dating the Santorini eruption. *Scientific Reports* 8: 11841.
- Ehrlich Y, Regev L, Boaretto E. 2021. Discovery of annual growth in a modern olive branch based on carbon isotopes and implications for the Bronze Age volcanic eruption of Santorini. *Scientific Reports* 11:704.
- Friedrich WL, Bernd Kromer B, Friedrich M, Heinemeier J, Pfeiffer T, Talamo S. 2006. Santorini eruption radiocarbon dated to 1627–1600 B.C. *Science* 312:548.
- Frisén J. 2016. Neurogenesis and gliogenesis in nervous system plasticity and repair. *The Annual Review of Cell and Developmental Biology* 32:127–141.
- Graven HD. 2015. Impact of fossil fuel emissions on atmospheric radiocarbon and various applications of radiocarbon over this century. *Proceedings of the National Academy of Sciences USA* 112(31):9542–9545.
- Grimm D. 2008. The mushroom cloud's silver lining. *Science* 321:1434–1437.
- Gruber N, Clement D, Carter BR, Feely RA, van Heuven S, Hoppema M, Ishii M, Key RM, Kozyr A, Lauvset SK, Monaco CL, Mathis JT, Murata A, Olsen A, Perez FF, Sabine CL, Tanhua T, Wanninkhof R. 2019. The oceanic sink for anthropogenic CO_2 from 1994 to 2007. *Science* 363:1193–1199.

- Hajdas I, Jull AJT, Huysecom E, Mayor A, Renold M-A, Syna H-A, Hatté C, Hong W, Chivall D, Beck L, Liccioli L, Fedi M, Friedrich R, Maspero F, Sava T. 2019. Radiocarbon dating and the protection of cultural heritage. *Radiocarbon* 61(5):1133–1134.
- Hamady LL, Natanson LJ, Skomal GB, Thorrold SR. 2014. Vertebral bomb radiocarbon suggests extreme longevity in white sharks. *PLoS ONE* 9(1):e84006.
- Hodge E, McDonald J, Fischer M, Redwood D, Hua Q, Levchenko V, Drysdale R, Waring C, Fink D. 2011. Using the ¹⁴C bomb pulse to date young speleothems. *Radiocarbon* 53(2):345–357.
- Hua Q, Barbetti M, Rakowski AZ. 2013. Atmospheric radiocarbon for the period 1950–2010. *Radiocarbon* 55(4):2059–2013.
- Huttner HB, Bergmann O, Salehpour M, Rácz A, Tatarishvili J, Lindgren E, Csonka T, Csiba L, Hortobágyi T, Méhes G, Englund E, Solnestam BW, Zdunek S, Scharenberg C, Ström L, Stahl P, Sigurgeirsson B, Dahl A, Schwab S, Possnert G, Bernard S, Kokaia Z, Lindvall O, Lundberg J, Frisén J. 2014. The age and genomic integrity of neurons after cortical stroke in humans. *Nature Neuroscience* 17(6):801–803.
- Huysecom E, Hajdas I, Renold M-A, Synal H-A, Mayor A. 2017. The “enhancement” of cultural heritage by AMS dating: ethical questions and practical proposals. *Radiocarbon* 59(2): 559–563.
- Hyvönen MT, Spalding KL. 2014. Maintenance of white adipose tissue in man. *The International Journal of Biochemistry and Cell Biology* 56:123–132.
- IPCC. 2013. *Climate Change 2013: The Physical Science Basis*. Contribution of Working Group I to the Fifth Assessment Report of the Intergovernmental Panel on Climate Change. Eds: Stocker TF, Qin D, Plattner GK, Tignor M, Allen SK, Boschung J, Nauels A, Xia Y, Bex V, Midgley PM. Cambridge University Press, Cambridge, United Kingdom and New York, NY, USA. 1535 p. See also: <https://www.ipcc.ch/report/ar5/wg1/>
- Keeling RF. 2008. Recording Earth’s vital signs. *Science* 319:1771–1772. See also <https://scripps.ucsd.edu/programs/keelingcurve/>.
- Kjeldsen H, Heinemeier J, Heegaard S, Jacobsen C, Lynnerup H. 2010. Dating the time of birth: a radiocarbon curve for human eye-lens crystalline. *Nuclear Instruments and Methods in Physics Research B* 268:1303–1306.
- Kutschera W. 2020. On the enigma of dating the Minoan eruption of Santorini. *Proceedings of the National Academy of Sciences USA* 117(16):8677–8679.
- Levin I, Hammer S, Kromer B, Preunkert S, Weller R, Worthy DE. 2022. Radiocarbon in global tropospheric carbon dioxide. *Radiocarbon*. doi: 10.1017/RDC.2021.102.
- Levin I, Heshshaimer V. 2000. Radiocarbon—a unique tracer of global carbon cycle dynamics. *Radiocarbon* 42(1):69–80.
- Libby WF, Berger R, Mead JF, Alexander GV, Ross JF. 1964. Replacement rates for human tissue from atmospheric radiocarbon. *Science* 146:1170–1172.
- Lynnerup N, Kjeldsen H, Heegaard S, Jacobsen C, Heinemeier J. 2008. Radiocarbon dating of the human eye lens crystallines reveal proteins without carbon turnover throughout life. *PLoS ONE* 1:e1529.
- Markowska M, Fohlmeister J, Treble PC, Baker A, Andersen MS, Hua Q. 2019. Modelling the ¹⁴C bomb-pulse in young speleothems using a soil carbon continuum model. *Geochimica et Cosmochimica Acta* 261:342–367.
- McCormac FG, Hogg AG, Higham TFG, Lynch-Stieglitz J, Broecker WS, Baillie MGL, Palmer J, Xiong L, Pilcher JR, Brown D, Hoper ST. 1998. Temporal variation in the interhemispheric offset. *Geophysical Research Letters* 25(9): 1321–1324.
- Münnich KO, Vogel JC. 1958. Durch Atomexplosionen erzeugter Radiokohlenstoff in der Atmosphäre. *Naturwissenschaften* 45(14): 327–329.
- Nielsen J, Hedeholm RB, Heinemeier J, Bushnell PG, Christiansen JS, Olsen J, Bronk Ramsey C, Brill RW, Simon M, Steffensen KF, Steffensen JF. 2016. Eye lens radiocarbon reveals centuries of longevity in the Greenland shark (*Somniosus microcephalus*). *Science* 353:702–704.
- Nydal R, Lövseth K. 1965. Distribution of radiocarbon from nuclear tests. *Nature* 206: 1029–1031.
- Ong JLL, Meekan MG, Hsu HH, Fanning LP and Campana SE. 2020. Annual bands in vertebrae validated by bomb radiocarbon assays provide estimates of age and growth of whale sharks. *Frontiers in Marine Science* 7:188.
- Pearson CL, Brewer PW, Brown D, Heaton TJ, Hodgins GWL, Jull AJT, Lange T, Salzer MW. 2018. Annual radiocarbon record indicates 16th century BCE date for the Thera eruption. *Science Advances* 4:eaar8241.
- Peters GP, Le Quéré C, Andrew RM, Canadell JG, Friedlingsten P, Ilyina T, Jackson RB, Joos F, Korsbakken JI, McKinley GA, Sitch S, Tans P. 2017. Towards real-time verification of CO₂ emissions. *Nature Climate Change* 7(12): 848–850.
- Quarta G, D’Elia M, Braione E, Calcagnile L. 2019. Radiocarbon dating of ivory: potentialities and limitations in forensics. *Forensic Science International* 299:114–118.
- Rafter TA, Ferguson GJ. 1957. “Atom bomb effect” – recent increase of carbon-14 content of atmosphere and biosphere. *Science* 126:557–558.
- Rinyu L, Janovics R, Molnar M, Kisvaerday Z, Kemeny-Beke A. 2020. Radiocarbon map of a

- bomb-peak labeled human eye. *Radiocarbon* 62(1):189–196.
- Salehpour M, Håkansson K, Possnert G. 2015. Small sample accelerator mass spectrometry for biomedical applications. *Nuclear Instruments and Methods in Physics Research* 361:43–47
- Seltzer AM, Bekaert DV, Barry PH, Durkin KE, Mace EK, Aalseth CE, Zappala JC, Mueller P, Jurgens B, Kulongoski JT. 2021. Groundwater residence time estimates obscured by anthropogenic carbonate. *Science Advances* 7: eabf3503.
- Shi Z, Allison SD, He Y, Levine PA, Hoyt AM, Beem-Miller J, Zhu Q, Wieder WR, Trumbore S, Randerson JT. 2020. The age distribution of global soil carbon inferred from radiocarbon measurements. *Nature Geoscience* 13:555–559.
- Slotta F, Wacker L, Riedel F, Heußner K-U, Hartmann K, Helle G. 2021. High-resolution ¹⁴C bomb peak dating and climate response analyses of subseasonal stable isotope signals in wood of the African baobab – a case study from Oman. *Biogeosciences* 18:3539–3564.
- Spalding KL, Arner E, Westermark PO, Bernard S, Buchholz BA, Bergmann O, Blomqvist L, Hoffstedt J, Näslund E, Britton T, Concha H, Hassan M, Rydén M, Frisén J, Arner P. 2008. Dynamics of fat cell turnover in humans. *Nature* 453:783–787.
- Spalding KL, Bergmann O, Alkass K, Bernard S, Vial C, Buchholz BA, Possnert G, Mash DC, Druid H, Frisén J. 2013. Dynamics of hippocampal neurogenesis in adult humans. *Cell* 153: 1219–1227.
- Spalding KL, Bhardwaj RD, Buchholz BA, Druid H, Frisén J. 2005. Retrospective birth dating of cells in humans. *Cell* 122:133–143.
- Steier P, Liebl J, Kutschera W, Wild EM, Golser R. 2017. Preparation methods of µg carbon samples for ¹⁴C measurements. *Radiocarbon* 59(3): 803–814.
- Stewart DN, Lango J, Nambiar KP, Falso MJ, FitzGerald PG, Rocke DM, Hammock BD, Buchholz BA. 2013. Carbon turnover in water-soluble protein of the adult human lens. *Molecular Vision* 19: 463–475.
- Stuiver M, Braziunas TF. 1998. Anthropogenic and solar components of hemispheric ¹⁴C. *Geophysical Research Letters* 25(3):329–332.
- Suess HE. 1955. Radiocarbon concentration in modern wood. *Science* 122:415–417.
- Trumbore S. 2009. Radiocarbon and soil carbon dynamics. *Annual Review of Earth and Planetary Science* 37:47–66.
- Uno KT, Quade J, Fisher DC, Wittenmyer G, Douglas-Hamilton I, Andanje S, Omondi P, Litoroh M, Cerling TE. 2013. Bomb-curve radiocarbon measurement of recent biological tissues and applications to wildlife forensics and stable isotope (paleo)ecology. *Proceedings of the National Academy of Sciences USA* 110(29): 11736–11741.
- van Vuuren DP, Edmonds J, Kainuma M et al. 2011. The representative concentration pathways: an overview. *Climate Change* 109(1–2):5–31.
- Wang N, Shen C, Sun W, Ding P, Zhu S, Yi W, Yu Z, Sha Z, Mi M, He L, Fang J, Liu K, Xu X, Druffel ERM. 2019. Penetration of bomb ¹⁴C into the deepest ocean trench. *Geophysical Research Letters* 46:5413–5419.
- Warren PM. 2006. The date of the Thera eruption in relation to Aegean-Egyptian interconnections and the Egyptian historical chronology. In: Czerny E, Hein I, Hunger H, Melman D, Schwab A, editors. *Timelines: studies in honour of Manfred Bietak. Orientalia Lovaniensia* 149. Leuven (Belgium): Peters. Vol. II. p. 305–321.
- Wasser SK, Brown L, Mailand C, Mondol S, Clark W, Laurie C, Weir BS. 2015. Genetic assignment of large seizures of elephant ivory reveals Africa's major poaching hotspots. *Science* 349:84–87.
- Wild E, Golser R, Hille P, Kutschera W, Priller A, Puchegger S, Rom W, Steier P, Vycudilik W. 1998. First ¹⁴C results from archaeological and forensic studies at the Vienna Environmental Research Accelerator. *Radiocarbon* 40(1): 273–281.
- Wild EM, Kutschera W, Meran A, Steier P. 2019. ¹⁴C bomb peak analysis of African elephant tusks and its relation to CITES. *Radiocarbon* 61(5): 1619–1624.
- Worden AZ, Follows MJ, Giovannoni SJ, Wilken S, Zimmerman AE, Keeling PJ. 2015. Rethinking the marine carbon cycle: Factoring in the multifarious lifestyles of microbes. *Science* 347:1257594.
- Yeung MSY, Zdunek S, Bergmann O, Bernard O, Salehpour M, Alkass K, Perl S, Tisdale J, Possnert G, Brundin L, Druid H, Frisén J. 2014. Dynamics of oligodendrocyte generation and myelination in the human brain. *Cell* 159:766–774.